Research Article
Open Access

Engineering photo cross-linked porous network for efficient and selective removal of toxicants from wastewater

Abstract

This article delineates the UV curable synthesis of an organogel based on thiol-norbornene click chemistry. Characterisations of the material are accomplished by standard analytical and spectroscopic techniques. Rheological measurements suggest the presence of elasticity, which is one of the characteristic features of a gel system. The organogel is found to be mechanically and thermally stable. In particular, the gel shows excellent efficiency towards the removal of cationic dyes from aqueous phase. Additionally, the adsorption results fit with pseudo second order kinetics as well as Langmuir adsorption isotherm model with good correlation. DFT calculations suggest the favourable interaction energy between the dyes and the gel as the defining parameter for the selective uptake of cationic dyes by the gel. To the best of our knowledge, this is the first report unfolding the excellent efficiency of norbornene based photo cross-linked network towards removal of toxic dyes that are regularly discharged from textile and paint industries. Further, minimum water uptake during dye removal process keeps maximum amount of water available for future usage thereby making it an inexpensive material that has potential applications in toxic organic dye containing wastewater treatment.

Volume 2 Issue 2 - 2019

Sayantani Bhattacharya, Ajith Nair, Arijit Bag, Pradip Kumar Ghorai, Raja Shunmugam
Department of Chemical Sciences, India

Correspondence: Raja Shunmugam, Polymer Research Centre, Centre for Advanced Functional Materials, Department of Chemical Sciences, Indian Institute of Science Education and Research Kolkata, Mohanpur, West Bengal, 741246, India, Email sraja@iiserkol.ac.in

Received: May 11, 2019 | **Published:** June 04, 2019

Introduction

Direct discharge of dye-containing effluents into waterways by textile and printing industries is one of the major contributors to aquatic pollution because of the high toxicity and carcinogenicity of organic dyes.[1–4] In addition, the intense colour of the dyes hinders sunlight penetration, thereby causing great harm to aquatic organisms.[5–7] Contamination of water by toxic dyes is a major threat to both aquatic lives and mankind as it is associated with several risk factors.8,9 Thus, it is absolutely necessary to remove the toxicants from contaminated water for sustainability of life on earth.[10–15]

The limitations of several physical, chemical and biological approaches that are traditionally followed to remove dyes from wastewater arise from their exorbitant price, harsh route of synthesis and lack of flexibility.[16,17] Additionally, the adsorbent that finds application in wastewater treatment must be non-toxic, preferentially biocompatible, in order to eliminate any secondary pollution. In this regard, usage of polymeric gels may be considered as an alternative approach to decontaminate tainted water.[18–20] In recent years, many reports focus on the evolution of biopolymers as the potential adsorbents for their environmental compatibility, ease of synthesis as well as low cost. Norbornene based polymers are incredibly used in the field of drug delivery for a very long time because of its biocompatibility and extraordinary functional group tolerance.[21] We believe that the efficiency of biocompatible norbornene based cross-linked networks towards removal of toxic dyes has not been investigated so far.

The development of "click chemistry" approach, first described by Kolb et al.,[22] for the synthesis of advanced functional materials has opened up a new era in the field of synthetic organic chemistry. As pointed by Kolb, the click reactions are easy to execute, orthogonal and can be carried out at ambient conditions in environmentally benign solvents.[22] Though, a series of reactions were referred as click reactions in the initial days, only a few of them had drawn major attention because of their simplicity. These include Cu (I) mediated Huisgen reaction, metal free dipolar cycloaddition, thiol-ene, thiol-yne reactions, etc. Similarly, thiol-ene reactions are in the literature for more than a century, but recently received attention due to their resemblance with click reactions.[23–31] Several inherent aspects of thiol-ene reactions have made them a versatile platform for material synthesis. These reactions can be mediated by various ways such as, through radical pathway, catalytic pathway or by neucleophiles, acids or bases, etc.[28–32] Various-enes ranging from substituted, unsubstituted to strained olefins can serve as potential substrates for these reactions. However, their order of reactivity is primarily dependent on the degree of substitution.[33,34] Ideally, any thiols can undergo this reaction but the kinetics of reaction depends of the type of cleavage it brings about. Further, both heat and light can be used as mediators in thiol-ene reaction.[35] Photo-initiation is particularly advantageous compared to thermal one as the product can be easily modulated by tuning the light intensity.[36] The photo-initiated thiol-ene reaction is essentially a step-growth polymerisation process which results in highly uniform structures.36 The photoinduced thiol-norbornene click reaction proceeds in stoichiometric ratio that eliminates the scope of homopolymerisation.[37,38] This is a powerful reaction process due to its simplicity, versatility, insensitiveness to ambient oxygen and water and are reported to yield regioselectively single product.[35] The resultant thiol-norbornene photo cross-linked gels find great deal of application in various fields such as tissue engineering, cell culture, just to mention a few.[35, 39,40]

This work delineates the design and synthesis of photoinitiated thiol-norbornene click based organogel. The material exhibits good thermal and mechanical stability along with excellent elastic behaviour which is the characteristic feature of a gel. Further, the as-synthesized material has the ability to uptake a range of solvents (DMSO, DMF, DCM and chloroform) but has not swelled in water as suggested by solvent uptake analysis. Further, it is able to remove rhodamine B, methylene blue dyes from aqueous phase. Rhodamine B is known to be carcinogenic and methylene blue, although not strongly hazardous, has potential harmful effects. To the best of our knowledge, this is the first thorough investigation on the utility of norbornene based photo-cross-linked materials to remove toxic cationic dyes from water.

Experimental section

Materials: Furan, maleic anhydride, pentaerythritol tetrakis(3-mercaptopropionate) (PETMP), 2-hydroxy-4'-(2-hydroxyethoxy)-2-methylpropiophenone, 1-ethyl-3-(3-dimethylaminopropyl) carbodiimide hydrochloride (EDC), Ethanol, N,N-dicyclohexylcarbodiimide (DCC), 1,6-hexanediol, 4-dimethylaminopyridine (DMAP), Toluene, Hexane, deuterated chloroform ($CDCl_3$), deuterated dimethylsufoxide (DMSO-d_6) were purchased from Sigma-Aldrich. Potassium bicarbonate, sodium chloride, sodium bicarbonate were purchased from Merck and used without purification. Dichloromethane was distilled over calcium hydride under atmospheric pressure.

Synthesis of compound 1: Maleic anhydride 10g (102mmol) was dissolved in 80 mL toluene, stirred for 30minutes and filtered. Furan 8.32g (122.4 mmol) was added to the filtrate and left for stirring for 48hours. A white coloured precipitate was formed which was then filtered and washed using cold toluene to obtain the product (yield 82%).1H NMR (400MHz, DMSO-d_6) δ 3.2 (s, 2H), 5.42 (s, 2H), 6.54 (s, 2H);^{13}C NMR (100 MHz, DMSO-d_6) δ 49.2, 81.52, 137.40, 171.48.

Synthesis of compound 2: Compound 1, 8g (48mmol) was dissolved in 30mL of dry DCM. Dry ethanol 3.36mL (57.6mmol) was then added to the reaction mixture at room temperature under nitrogen atmosphere. After that, DMAP 0.58g (4.8mmol) was added to the solution and stirred overnight. Then, the reaction mixture was concentrated and precipitated from hexane: ether solution. Purification was carried out by re-crystallisation in DCM/Hexane to obtain a white coloured pure product (yield 57%).1H NMR (400MHz, DMSO-d_6) δ 1.23 (s, 3H), 2.84 (d, 2H), 4.08 (q, 2H), 5.21 (s, 2H), 6.43 (m, 2H), 12.3 (br s, 1H); 13C NMR (100 MHz, DMSO-d6) δ 13.51, 46.27, 60.04, 79.87, 136.41, 171.02, 171.10.

Synthesis of compound 3: Compound 2, 4g (18.9mmol) along with 1, 6-hexanediol 0.74 g (6.32mmol) and DMAP 0.24 g (1.9mmol) were dissolved in dry DCM under inert (nitrogen) condition. Subsequently, the reaction mixture was cooled at 0 ^{o}C and EDC 3.6g (18.8mmol) was added to the reaction mixture. The mixture was then allowed to reach room temperature and stirred for next 12 hours. After that, the solution was washed with 10% $KHSO_4$, saturated $NaHCO_3$ and saturated NaCl solutions, respectively. The solution was then dried using anhydrous Na_2SO_4 and concentrated by rotary evaporation. Pure product was obtained by column chromatography as light yellow liquid (yield 65%).[1] H NMR (400MHz, $CDCl_3$) δ 1.26 (t, 3H), 1.31-1.38 (m, 4H), 1.56-1.7 (m, 4H), 2.81 (s, 4H), 4.02-4.19 (m, 8H), 5.21 (m, 2H), 5.25 (m, 2H), 6.42 (s, 4H); 13C NMR (100 MHz, CDCl3) δ 13.82, 25.24, 27.89, 46.83, 46.89, 60.81, 65.02, 80.52, 136.84, 171.31, 171.35. MALDI for C26H34O10; calculated [M+Na+] is 529.20, observed 529.22m/z.

Synthesis of the gel: To prepare the chemically cross-linked gel, first the compound 3 was dissolved in DCM in a vial. To this solution, pentaerythritol tetrakis(3-mercaptopropionate) (PETMP) and 1 wt% of the photoradical generator (2-hydroxy-4'-(2 hydroxyethoxy)-2-methylpropiophenone) were added. The mixture was then exposed to UV light at room temperature for 30 minutes. After 30 minutes, formation of a gel was observed. It was then washed repeatedly by DCM to ensure complete removal of any unreacted monomer, cross-linker and photoinitiator. The material was dried in vacuum prior further analysis.

Solvent uptake analysis: The ability of the gel to swell in different solvents was studied gravimetrically at room temperature. Measured amount of the dried gel was taken in a vial. To that, different solvents were added and the vial was left undisturbed for 24 hours to reach equilibrium. Thereafter, the swelled gel was taken out and the excess solvent at the surface was carefully removed by wiping with a tissue paper and weighed again. Three sets of measurements were carried out for each sample. The swelling ratio (in %) was calculated using the following formula expressed in Eq. 1.

$$Swelling\ ratio\ (in\ \%) = \frac{ws - wd}{wd} \times 100 \qquad (Eq.1)$$

Where w_s and w_d are the mass of swollen gel and dry gel respectively.

Dye removal studies: The removal of dyes by the gel network was investigated by UV-Vis spectroscopic technique. Each dye removal experiment was carried out thrice to probe the dye adsorption by the gel system. For the isotherm experiments, 0.2g of the gel was added to the various dye solutions of preferred concentration (0.47mg/L to 47.9mg/L for rhodamine B and 0.32mg/L to 31.9mg/L for methylene blue) and the decrease in absorbance was observed with increase in time. However, for the kinetic experiments, dye concentrations were fixed at 0.1mM. Concentration of dye solution after adsorption was obtained by comparing the UV-vis absorbance with the appropriate calibration curve. The amount of dye absorbed per unit weight of the gel, qe (mg/g) was also calculated using the following formula expressed as Eq. 2,

$$q_e = \frac{Co - Ce}{m} V \qquad (Eq.2)$$

where C_0 is the initial concentration of dye in aqueous solution in mg/L and C_e is the equilibrium concentration of the dye in solution in mg/L. m is the mass of adsorbent in g and V is the volume of solution in L (Figure 1), (Figure 2A).

Results and discussion

With the aim of removing toxic dyes, we look forward to develop a material based on the fascinating photoinitiated thiol-norbornene click chemistry.[41] For that purpose, we have chosen compound 3 as the desired cross-linker which was synthesised simply by a three step process (Figure 1). Diels-Alder reaction was employed between furan and maleic anhydride in toluene to obtain compound 1, which was characterised by 1H and 13C NMR (Supplementary Figures 1 & 2). In the second step, compound 1 was treated with dry ethanol, DCC and DMAP in dry DCM. Compound 2 was purified by re-crystallisation. The –COOH peak at δ 12.3 ppm confirmed the formation of compound 2 (Suppplimentary Figures 3 & 4). The cross-linker was prepared by coupling reaction between 1, 6-hexanediol and compound 2, using EDC as the coupling agent. Purification was carried out by column chromatography in ethyl acetate/hexane. The product formation was confirmed by 1H NMR,[13] CNMR and by Mass spectrometry (Suppplimentary Figures 5–10). For the preparation of the gel, Cross-linker, photoinitiator and pentaerythritol tetrakis (3-mercaptopropionate) (PETMP) were dissolved in dry DCM and kept under UV light. The molar ratio of thiol to norbornene was varied from 1:2, 1.5:2 and 2:1 to fine-tune the cross-linking density. Very fast gelation was observed within 30 minutes for the feed ratio 1:2. Formation of gel was confirmed primarily by vial inversion method (Figure 2B). The study of viscoelastic property revealed formation of stronger gel with higher storage modulus (G') and loss modulus

Citation: Bhattacharya S, Nair A, Bag A, et al. Engineering photo cross-linked porous network for efficient and selective removal of toxicants from wastewater. *MOJ Research Review.* 2019;2(2):69–81. DOI: 10.15406/mojcrr.2019.02.00058

(G'') for this particular feed ratio (Suppplimentary Figure 11).[44] As higher storage modulus is directly related to the extent of cross-linking, we may conclude that this particular gel possesses highest cross-linking density.[44] Therefore, further studies were carried out with this material. The gel formation was further confirmed by FT-IR spectroscopy (Figure 3). In the FT-IR spectra, the S-H stretching frequency from the tetrathiol component (PETMP) at 2520cm^{-1} has diminished after gelation, indicating the consumption of thiols.

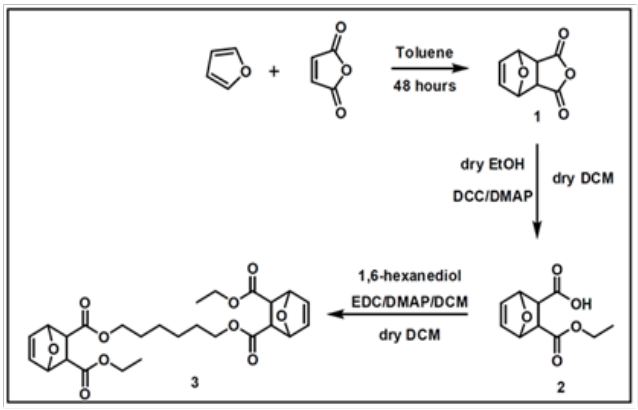

Figure 1 Synthesis scheme of the cross-linker 3**.**

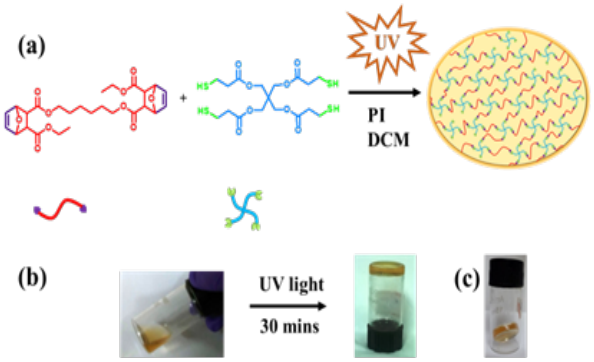

Figure 2 (A) Synthesis scheme of the gel; (B) Photographs of before and after photoirradiation; (C) Photograph of the gel.

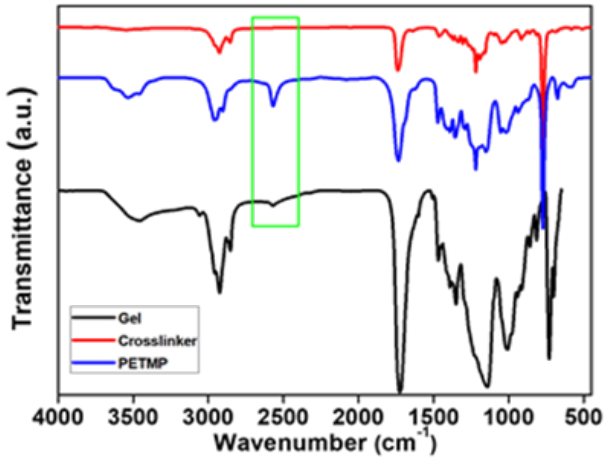

Figure 3 FT-IR spectra of the gel, crosslinker and PETMP. The decrease of peak intensity at 2520 cm^{-1} in the gel indicates consumption of thiols during gelation.

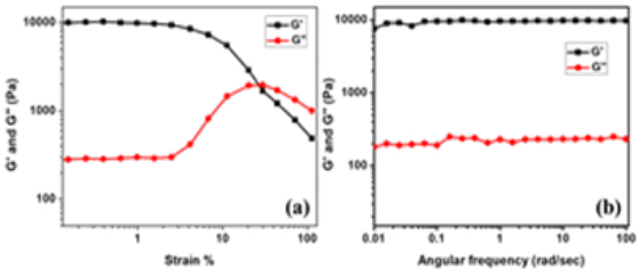

Figure 4 (A) Storage modulus (G') and loss modulus (G'') of the gel versus strain sweep. (B) Storage modulus (G') and loss modulus (G'') of the gel versus frequency sweep (strain 1%).

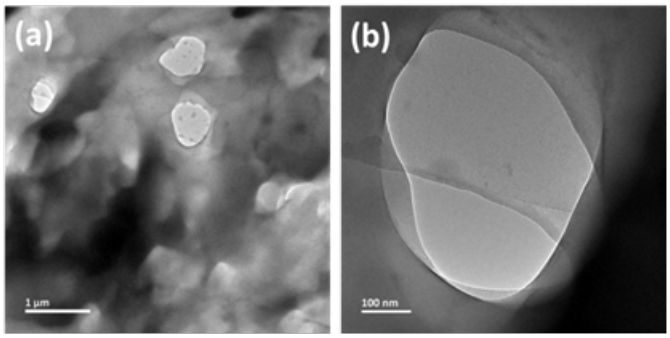

Figure 5 TEM images of the gel after ultra-microtome at scale bar (A) 1µm and (B) 100 nm respectively.

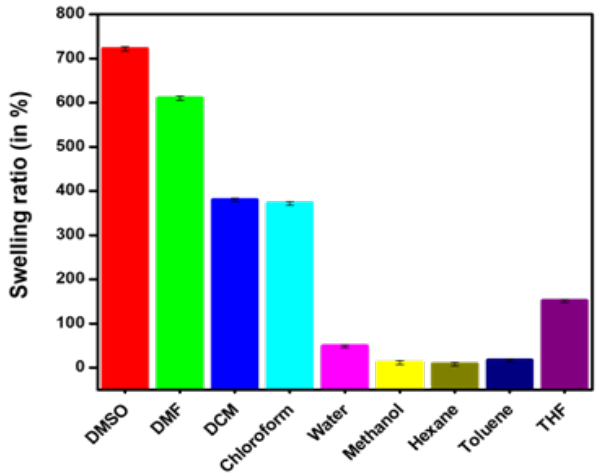

Figure 6 Solvent uptake analysis of the gel in various solvents.

The newly formed C-S bond in the gel was confirmed by Raman spectra (Suppplimentary Figure 8). To recognise the connectivity in the gel, cross-polarisation (CP),[13] C MAS spectrum was also recorded (Suppplimentary Figure 9), where the decrease of olefin signal at 136.8ppm confirmed successful thiol-ene click reaction.

Rheological measurement was carried out at room temperature to study the viscoelastic properties of the covalently cross-linked network. Initially, the storage modulus (G') and the loss modulus (G'') were monitored versus strain % in order to obtain the linear viscoelastic regime and the linear viscoelastic region was observed up to 3%. Therefore, the frequency sweep experiment was performed at a constant strain 1% which is below the deformation limit of the gel. For an ideal liquid, the value of G' that indicates the propensity

of a deformed material to re-gain its actual shapes zero whereas, for an ideal solid, the value of G'' that implies the tendency of a material to flow is zero.[42,43] As shown in Figure 4, it is evident that for the as synthesized covalently cross-linked material, G'> G''. This indicates the presence of elastic property that is the characteristic feature of gel. It is observed that the storage modulus is highest (~9000 Pa) for the gel where the thiol-norbornene molar ratio is 1:2 and it is lowest (~2000 Pa) when the ratio is 2:1 (Suppplimentary Figure 11). Higher storage modulus indicates greater tendency of the material to store the deformation energy in elastic manner (Figure 4).[44]

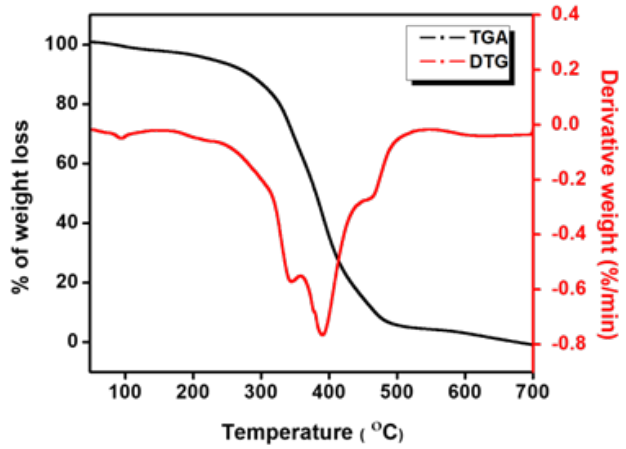

Figure 7 TGA and DTG curves of the gel at heating rate 10 °C/minute.

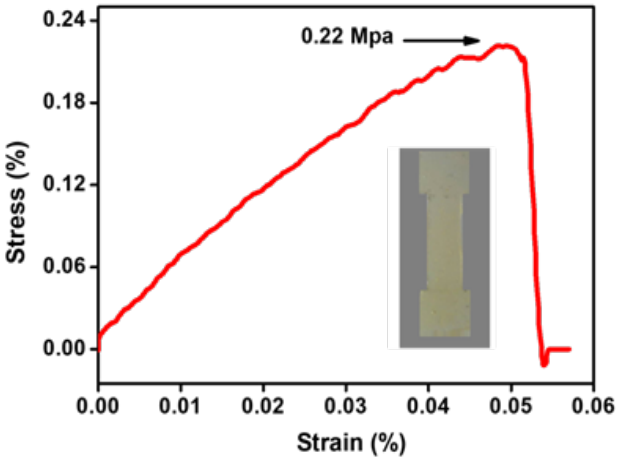

Figure 8 Tensile strength and Young's modulus of the gel.

To study the morphology of the organogel, FE-SEM analysis was carried out (Suppplimentary Figure 10). Morphology of the gel primarily depends on gelation mechanism, time and cross-linking density and also on solvents.[45,46] To get a deep insight of the porous nature, TEM analysis was carried out by using ultra microtome (Figure 5). It is clear that the covalently cross-linked gel possesses uniform porous nanostructure. The pore sizes were measured to be around 500nm, which is smaller than the traditional covalently cross-linked gels,[47] owing to the formation of highly cross-linked network structure with a very short period of time.[48]

The porous network as was observed from TEM analysis inspired us to explore the solvent uptake ability of the material at room temperature. For solvent uptake behaviour analysis, a range of solvents with varied polarity, such as hexane (dielectric constant, ε=1.88), toluene (ε=2.38), chloroform (ε=4.81), tetrahydrofuran (ε=7.58), dichloromethane (ε = 8.93), methanol (ε=32.7), N, N-Dimethylformamide (ε=36.7), dimethyl sulfoxide (ε=46.6) and water (ε=80.1) were employed. For quantification purpose, gravimetric method was adopted (Figure 6) and the % weight gain was calculated using (Eq.1). In general, the swelling capacity of a cross-linked network with various solvents primarily depends on solvent polarity and the nature of the cross-linked constituents (hydrophilic/hydrophobic). From the result it is evident that the gel is swelling favourably in both polar aprotic solvents (DMSO, DMF, DCM) with high dielectric constant (ε > 8) and non-polar solvent ($CHCl_3$) with relatively high dielectric constant (ε=4.8) compared to other non-polar solvents with lower dielectric constant and any polar protic solvent. The rationale behind higher solvent uptake by the gel can be attributed to the compatibility of the cross-linked network with the polarity of the solvent medium.[46] The porous network is found to swell favourably in aprotic solvents and the solvent uptake generally increases with increase in solvent polarity. Such dependence on polarity can be ascribed to the presence of polar groups, such as C=O, etc., which provides stabilization via Coulombic interaction. In contrast, the network does not swell significantly in polar protic solvents, such as water or methanol. This suggests that though polarity plays a decisive role in case of aprotic solvents, it is not the only determining factor behind solvent uptake. Further, this kind of behaviour closely resembles to that of polystyrene resins that uptake polar aprotic solvents but do not swell in polar protic solvents.[49,50] We believe that such unfavourable uptake of protic solvents may be due to the absence of any readily exchangeable ionic part in the network that are necessary to provide stabilization to protic solvents.

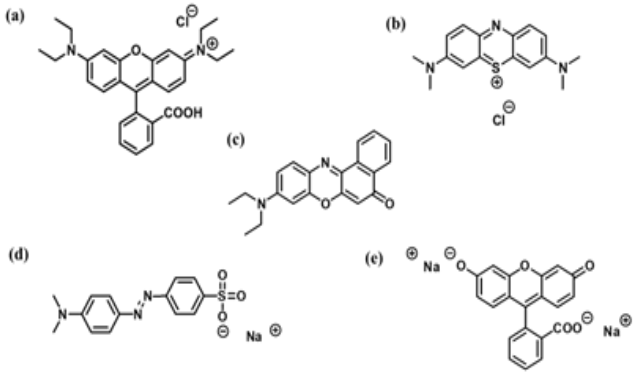

Figure 9 Chemical structures of the studied dyes (A) rhodamine B. (B) methylene blue. (C) nile red. (D) methyl orange and (E) fluorescein sodium.

A much desired property of a toxicant remover for practical usage lies in its capability to withstand high temperature as it should not degrade below the temperature of contaminated water. The thermal stability of the synthesised organogel was thus investigated by thermo gravimetric analysis (Figure 7). TGA thermogram shows a single step degradation. However, the first derivative plot (DTG) clearly displays three step thermal degradation pattern. The initial weight loss around 100 °C may be attributed to the loss of adsorbed water. Next, weight loss around 340 °C suggests degradation of the C-S bond present in the system.[51] Further, weight loss around 390°C reveals structural changes such as loss of carbonyl groups present in the cross-linked network and the degradation at 470 °C suggest cleavage of the C-O-C linkage.[52]

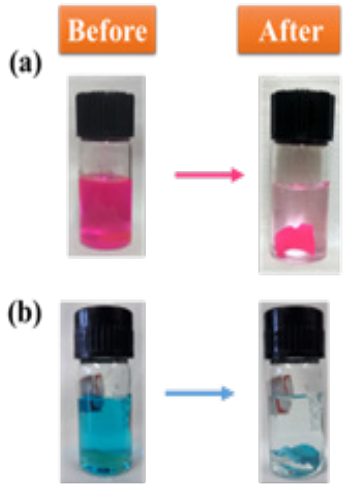

Figure 10 Photographs of the gel before and after removal of cationic dyes (A) rhodamine B and (B) methylene blue.

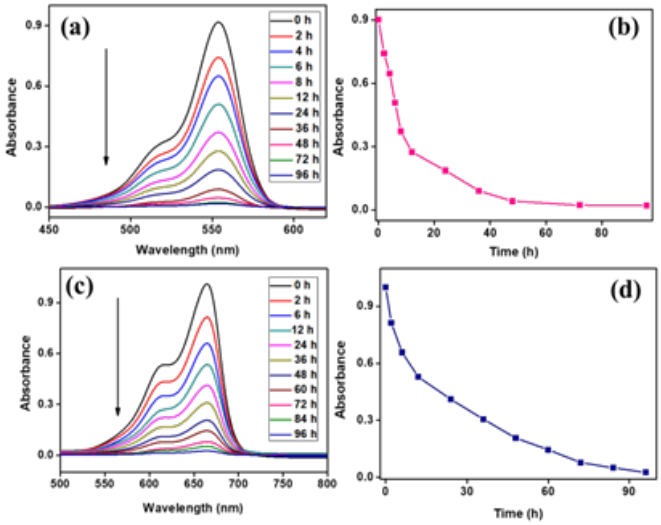

Figure 11 UV-Vis spectra of 0.1 mM cationic dyes solution after indicated time (A) rhodamine B and (C) methylene blue. plots of absorbance of (B) rhodamine B and (D) methylene blue with time.

Good mechanical stability is another important parameter for the practical usage of a toxicant remover. To investigate the toughness of the synthesised organogel, tensile stress-strain profile was evaluated. Although several reports on mechanical properties of organogels are available in literature,[53–60] norbornene based organogels are relatively less explored and demand attention. Recently, Cui et al demonstrated the mechanical properties norbornene based gels with PEG moiety for biological applications.[61] They have used thiol-ene click chemistry for the synthesis of the gel. In the present work, we have utilised photoinduced thiol-norbornene click chemistry for the preparation of the desired organogel. From the stress-strain profile (Figure 8), we observed that the tensile strength and Young's modulus of the material are 0.22MPa and 480kPa, respectively.

This is particularly noteworthy as the Young's modulus of the hydrogel that has been studied by Cui et al was 34kPa. Hence, from the study of mechanical properties, it can be inferred that a very rigid and hard organogel has been achieved successfully. Further, we believe that the observed rigidity by means of Young's modulus has aroused due to extensive connectivity in the network structure formed by the tetra-arm thiol moiety and norbornene based cross-linker upon UV irradiation. To the best of our knowledge, this type of hard organogels, by means of Young's modulus, resulted from photoinitiated thiol-norbornene click chemistry is being evaluated for the first time.

The fulfilment of initial parameters that are necessary for a cross-linked gel to be used as a toxicant remover motivated us to evaluate the dye removal capacity of the cross-linked gel (Figure 9). Aqueous solution of several widely used organic dyes such as, rhodamine B and methylene blue (both cationic), nile red (non-ionic), methyl orange and fluorescein sodium (both anionic) were used and the dye removal ability of the gel was probed by monitoring the time-dependent UV absorption of the dye solutions.

For the kinetic experiments, the UV absorption of a 0.1mM aqueous solution of cationic dye rhodamine B was initially recorded and thereafter, a 200mg of the gel was placed (Figure 10 A) in that solution. The absorbance of the dye solution was then monitored at different time intervals (Figure 11 A & B) and the difference between the initial and final UV intensity revealed the extent of dye absorption by the gel (Figure 10).

It was observed that almost 50% of the dye was removed within first 12hours. The absorbance was monitored for 4days to find the optimum capacity. In spite of the fact that the gel did not swell in water, it was able to remove the entire dye from water leaving the solution clear. To check the selectivity of the gel towards dyes, the same experiment was repeated with a variety of organic dyes.

For methylene blue, which is also a cationic dye (Figure 10B), a similar phenomenon was observed (Figure 11 C&D). The gel was able to eliminate the dye completely resulting in a clear solution. In case of nile red, which is non-ionic in nature, the gel was again able to remove the dye completely (Suppplimentary Figure 12).

However, for methyl orange and fluorescein, both of which are anionic, negligible change in UV spectra was observed indicating that the gel is not able to efficiently remove anionic dyes. As shown in Figure 12 B&D, negligible amount of fluorescein sodium was removed by the gel even after prolonged time while for methyl orange, a slight removal had taken place (Figure 12 A&C). These results indicate that the organogel was highly efficient to remove cationic dyes from the aqueous phase but not competent towards anionic dye removal.

Adsorption kinetics

In order to appraise the mechanism which governs the dye removal process, the kinetic data were fitted into the following pseudo-first-order (Eq. 3), pseudo-second-order (Eq. 4), and Weber-Morris intraparticle diffusion models (Eq. 5) and validity of the models were evaluated from corresponding correlation coefficients (R^2).[62]

$$\log(q_e - q_t) = \log q_e - \frac{k_1}{2.303} t \qquad \text{(Eq.3)}$$

$$\frac{t}{q_t} = \frac{1}{k_2 q_e^2} + \frac{t}{q_e} \qquad \text{(Eq.4)}$$

$$q_t = k_t + t\frac{1}{2} + C \qquad \text{(Eq.5)}$$

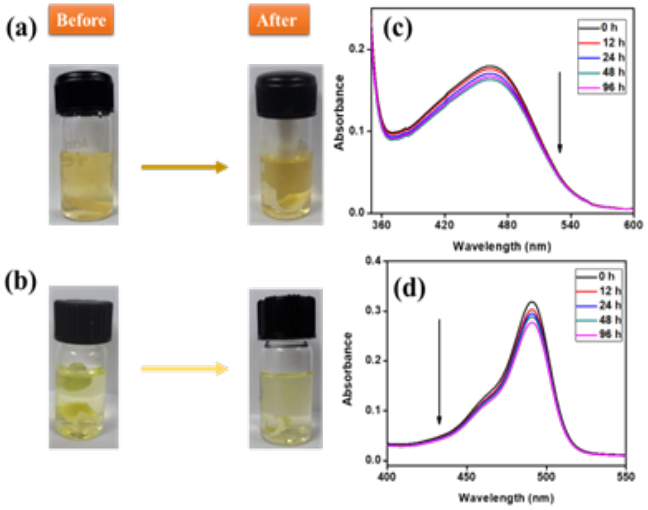

Figure 12 Photograph of anionic dye solutions (A) methyl orange and (B) fluorescein sodium before (0 h) and after (96 h); UV-Vis spectra of (C) methyl orange and (D) fluorescein sodium after the indicated time.

Where q_t and q_e are the amount of adsorbed dye (mg g^{-1}) at time t and at equilibrium and k_1 (h^{-1}) is the pseudo-first-order rate constant. k_2 (g mg^{-1} h^{-1}) is the pseudo-second-order rate constant, k_i is the intraparticle diffusion rate (mg g^{-1} h^{-1}) and C (mg g^{-1}) is the constant corresponding to the thickness of the boundary layer. All the above parameters were calculated from the slopes and intercepts of the linear plots of log (q_e - q_t) vs. t for pseudo-first-order, t/qt vs. t plots for pseudo-second-order and qt vs. $t^{1/2}$ plot for intraparticle diffusion model.

The results are depicted in Figure 13, 14 and Table 1. It is evident from the high degree of linearity that pseudo-second-order model (correlation coefficient R^2=0.997 for rhodamine B and 0.993 for methylene blue) describes the adsorption process better than pseudo-first-order model (correlation coefficient R^2=0.982 for rhodamine B and 0.965 for methylene blue) and intraparticle diffusion model (correlation coefficient R^2=0.799 for rhodamine B and 0.980 for methylene blue). Furthermore, the value obtained from pseudo-second-order model (2.40 mg g^{-1} for rhodamine B and 1.64 mg g^{-1} for methylene blue) is better comparable with the experimental data (2.38 mg g^{-1} for rhodamine B and 1.58 mg g^{-1} for methylene blue). The better fitting with pseudo-second-order kinetics model indicates that the dye adsorption by the gel results from chemisorptions.[63]

$$\frac{c_e}{q_e} = \frac{1}{bq_m} + \frac{c_e}{q_m}$$

To get a deeper insight of the dye adsorption type, two most commonly used adsorption models namely Langmuir model and Freundlich model were fit into the experimentally obtained isotherm data. The Langmuir isotherm model is based on the assumption that the adsorption of the adsorbent onto the adsorbate is monolayer. The linear form of Langmuir isotherm model can be expressed as:

$$R_L = \frac{1}{1 + bC_O}$$

where C_e is the equilibrium concentration of dye in mg L^{-1}, q_e is the amount of the dye adsorbed in mg g^{-1}, q_m is the monolayer adsorption capacity of the adsorbent in mg g^{-1} and b is Langmuir constant denoting to energy of adsorption; depicting the affinity between adsorbent and adsorbate.[63] The Langmuir isotherm is also expressed as the following dimensionless equilibrium parameter (R_L),

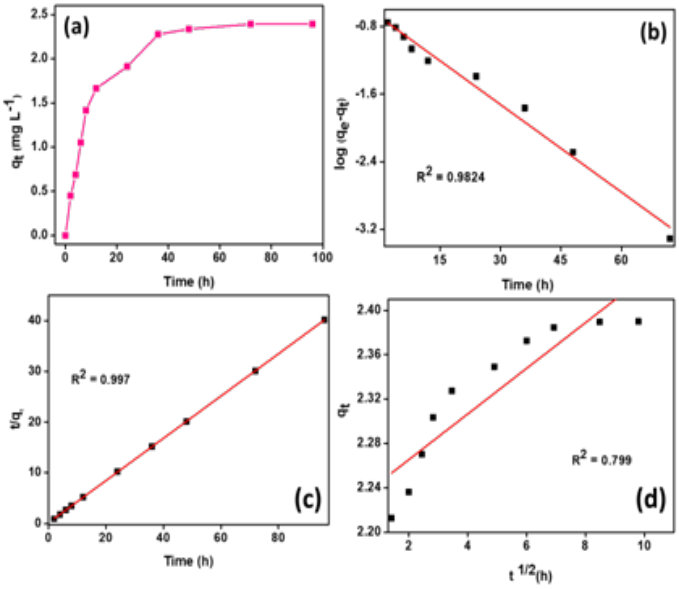

Figure 13 (A) Time dependent rhodamine B sorption on the gel. kinetic curves of (B) pseudo-first-order. (C) pseudo-second-order and (D) intra-particle diffusion model.

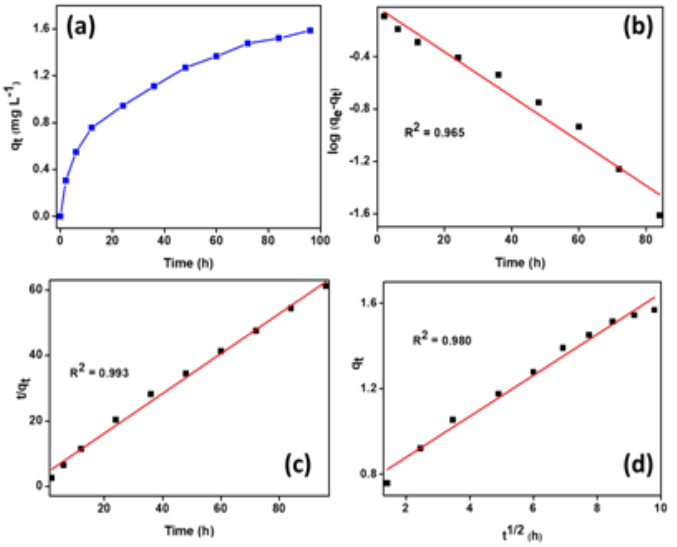

Figure 14 (A) Time dependent methylene blue sorption on the gel. kinetic curves of (B) pseudo-first-order. (C) pseudo-second-order and (D) intra-particle diffusion model.

where C_0 is the initial concentration of the dye in mg L^{-1} and the value specifies the type of adsorption. If R_L=0, it indicates that the adsorption is irreversible. If, 0< R_L<1, the adsorption is favourable, R_L=1 indicates linear adsorption and R_L> 1 indicates unfavourable adsorption.[62]

The Freundlich isotherm model is an equation based on adsorption on a heterogeneous surface. The equation can be written as following:

$$In\, q_e = In\, k_f + \frac{1}{n} In\, C_e$$

Table 1 Kinetics parameters of adsorption of rhodamine B and methylene blue on the gel

Dye	Pseudo-first order model	Pseudo-second order model	Intra-particle diffusion model
rhodamioe B	R^2=0.982	R^2=0.997	R^2=0.799
	q_e=0.21 mg g^{-1}	q_e=2.40 mg g^{-1}	C=0.021 mg g^{-1}
	K1=0.079h^{-1}	K2=1.3 g mg h^{-1}	K1=2.22 mg g-1 h^{-1}
methylene blue	R^2=0.965	R^2=0.993	R^2=0.980
	q_e=0.95 mg g^{-1}	q_e=1.64 mg g^{-1}	C=0.0686 mg g^{-1}
	K1=0.039h^{-1}	K2=0.0938g mg h^{-1}	K_i=0.095mg g h^{-1}

where n is the Freundlich constant and k_f is the constant related to the adsorption capacity. The Langmuir and Freundlich isotherms are represented in Figure 15 & 16 and Table 2. The correlation coefficient (R^2) determined for both the dyes namely, rhodamine B and methylene blue, from the Langmuir model (0.998 for rhodamine B and 0.997 for methylene blue) was much higher than that of Freundlich model (0.883 for rhodamine B and 0.884 for methylene blue), signifying that the experimental data shows better compliance with Langmuir model and the R_L value is also 0.0012-0.114 for rhodamine B and 0.0075-0.08 for methylene blue, which lies between 0 to 1, suggesting favourable adsorption of the cationic dyes by the gel.

Table 2 Isotherm parameters of sorption of rhodamine B and methylene blue on the gel

Adsorption Isotherm	rhodamine	methylene blue
Langmuri model	R^2=0.982	R^2=0.997
	qm=2.48 mg g	qm=1.64 mg g
	b=16.12 Lmg	b=41.6 L mg g
	R_L=0.0012-0.114	R_L=0.0075-0.08
Freundich model	R^2=0.883	R^2=0.884
	Kf=3.46	Kf=2.40
	n=1.84	n=2.52

The uniqueness of this piece of work is that, we have developed a system which is not swelling in aqueous medium yet it is efficient to remove the selective toxicants which are dissolved in water. This is particularly of interest as an ideal toxicant remover must not take up water itself during purification process so that the maximum amount of water is available for further use.

To understand the nature of interaction of different dyes with our gel, we performed ab-initio quantum computation in density functional theory (DFT) regime. For this study GAUSSIAN 09 package was used.[64] Computation was done taking only a small portion of gel (two repeated units of gel). 6-311G basis was used with B3LYP functional.[65] Geometry optimization (Suppplimentary Figure 13) was performed without any negative frequency for different dyes, gel and gel-dye complex. Effect of solvation was included taking water as solvent. We calculated interaction energies of different complex formation. Computed results were presented in Table 3. These results suggest the presence of high ionic interaction energy between the dyes rhodamine B and methylene blue with the gel. We believe that this may be primarily responsible for their rapid removal from aqueous solution. On the contrary, relatively lower interaction energy between the gel and anionic dyes, i.e., methyl orange and fluorescein sodium resulted in their negligible uptake.

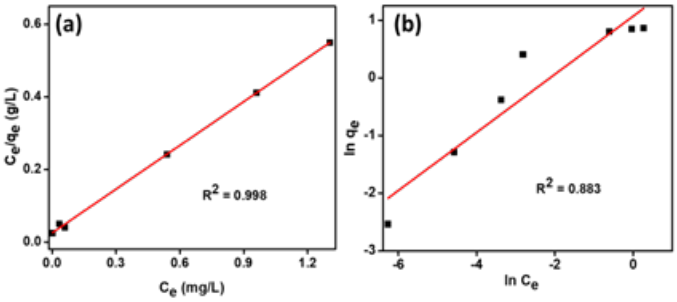

Figure 15 (A) Langmuir and (B) Freundlich isotherm model of rhodamine B sorption on the gel.

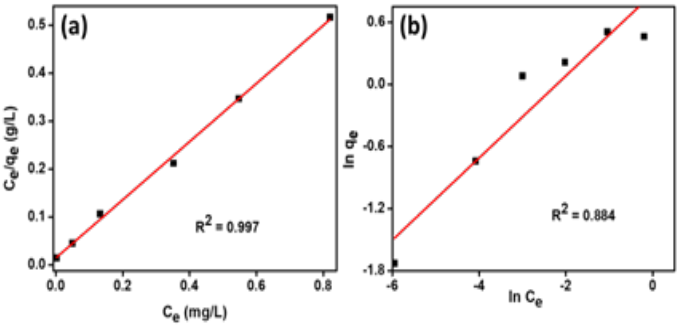

Figure 16 (A) Langmuir and (B) Freundlich isotherm model of methylene blue sorption on the gel.

Table 3 Interaction energies of different dyes with the gel

Indicator	Interaction energy (kcal/mol)	Predicted nature of interaction
rhodamine B	-844	Ionic interaction
methylene blue	-508	Ionic interaction
nile red	-298	Non-bonding interaction
methyl orange	-197	Non-bonding interaction
Fluorescein sodium	8.2	Repulsive interaction

The reusability of the material is of supreme importance for practical applications. Ethanol was found to be an effective eluent for the desorption of rhodamine B. The recyclability was investigated by monitoring the UV-Vis spectra of the dye solution. Equation S1 was used to calculate the removal efficiency of the system.[20]

Figure 17 depicts that the removal efficiency of the dye rhodamine B remains about 83% after initial 5th cycle, suggesting significant recyclability of the material for dye removal. The fairly good recyclability of the material can be attributed to its highly cross-linked network structure with good mechanical stability.

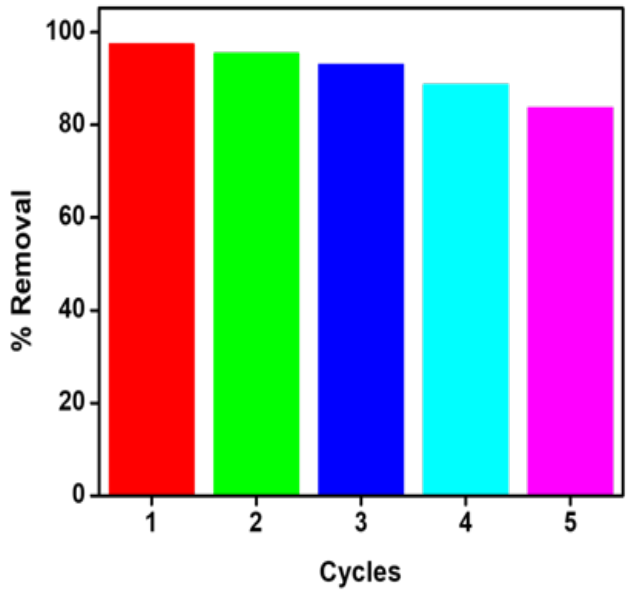

Figure 17 Reusability test for the dye rhodamine B upto five cycles.

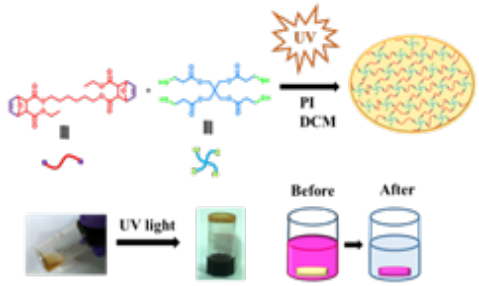

Figure 18 Engineering photo cross-linked porous network for efficient and selective removal of toxicants from wastewater.

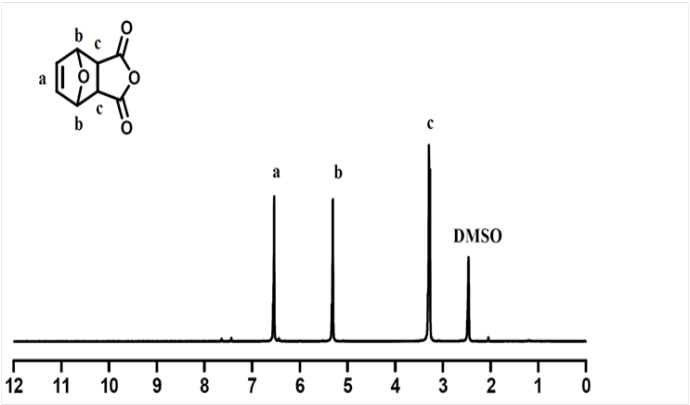

Figure S1 ^{1}H NMR spectrum of compound **1** in DMSO-d_6.

Table of content:

Engineering photo cross-linked porous network for efficient and selective removal of toxicants from wastewater

Experimental section:

Instrumentation techniques:

Nuclear Magnetic Resonance (NMR): The 1H NMR spectroscopy was carried out on a JEOL 400MHz spectrometer using $CDCl_3$ and DMSO-d_6 as solvents.^{1}H NMR spectra were calibrated to tetramethylsilane as internal standard (δ_H 0.00).

Fourier Transform Infra -Red (FT-IR): FT-IR spectra were obtained on FT-IR Perkin-Elmer spectrometer at a nominal resolution of 2cm^{-1}.

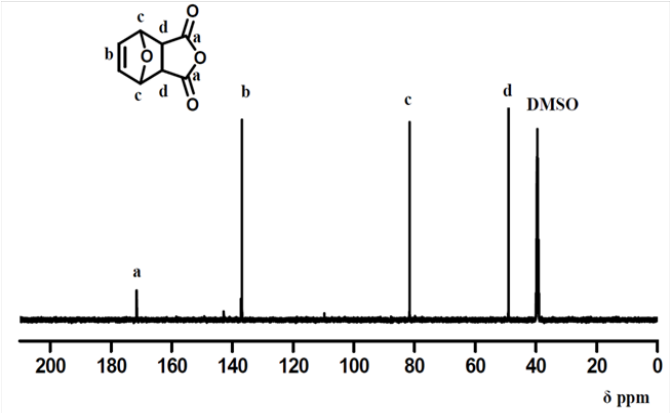

Figure S2 ^{13}C NMR spectrum of compound **1** in DMSO-d_6.

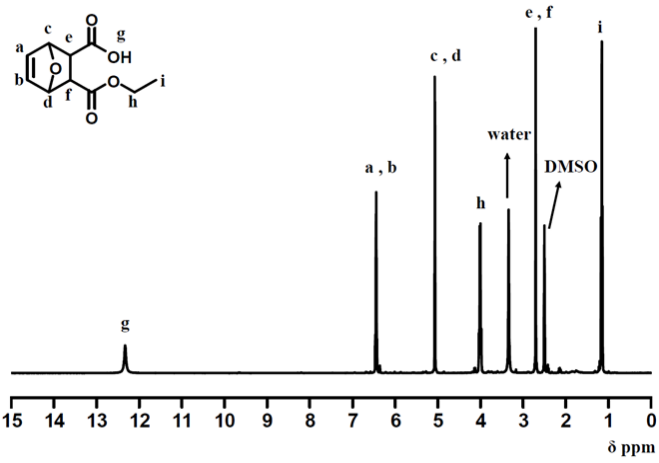

Figure S3 ^{1}H NMR spectrum of compound **2** in DMSO-d_6.

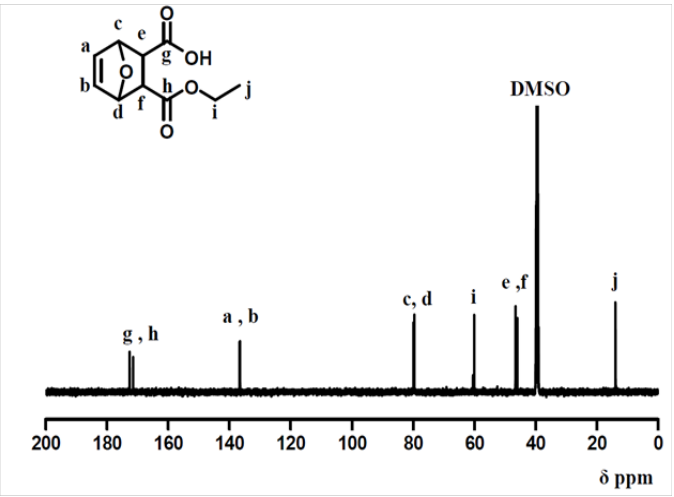

Figure S4 ^{13}C NMR spectrum of compound **2** in DMSO-d_6.

Matrix-Assisted Laser Desorption/Ionisation (MALDI-TOF): Positive mode electrospray ionization mass spectrometry (ESI-MS) was carried out on a Q-Tof Micro YA263 high resolution (Waters Corporation) mass spectrometer.

Raman Spectrometer: Micro-Raman spectrum was obtained from Raman Spectrometer, Horiba Jobin Yvon, HR 800 double grating.

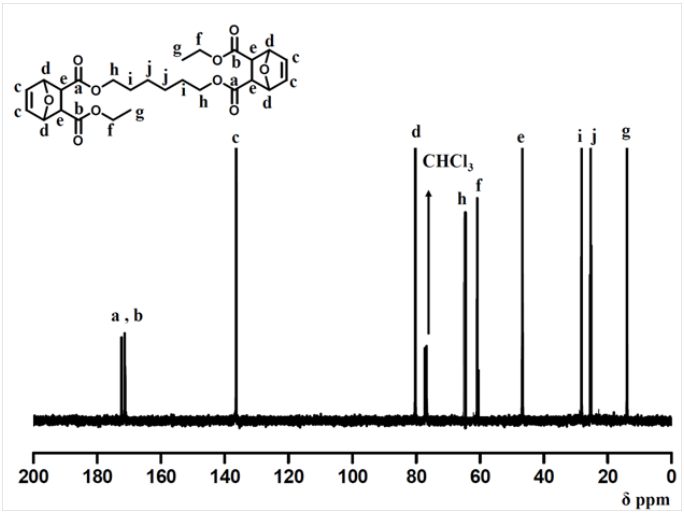

Figure S5 ^{1}H NMR spectrum of compound **3** in $CDCl_3$.

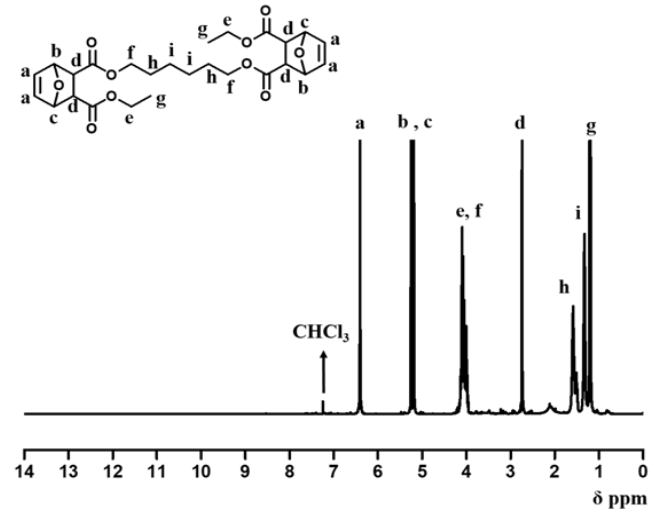

Figure S6 ^{13}C NMR spectrum of compound **3** in $CDCl_3$.

Rheometer: The rheological measurements were carried out on a TA-ARG2 rheometer using a steel parallel plate with 60 mm diameter at 25° C with 1.0 mm Gap spacing for all gel samples. The dynamic shear moduli (G′ and G″) were recorded in the linear viscoelastic regime at a strain of γ=1% as a function of angular frequency (0.1−100 rad/s).

UV-Vis Spectroscopy: UV-visible absorption measurements were carried out on U-4100 spectrophotometer; HITACHI spectrometer, with a scan rate of 500nm/min.

Scanning Electron Microscopy (SEM): High resolution SEM was performed on a Zeiss microscope; SUPRA 55VP-Field Emission Scanning Electron Microscope. High performance variable pressure FE-SEM with patented GEMINI column technology. Schottky type field emitter system, single condenser with crossover-free beam path. Resolution: 1.0nm at 15kV; 1.6nm at 1kV high vacuum mode. 2.0nm at 30kV at variable pressure mode.

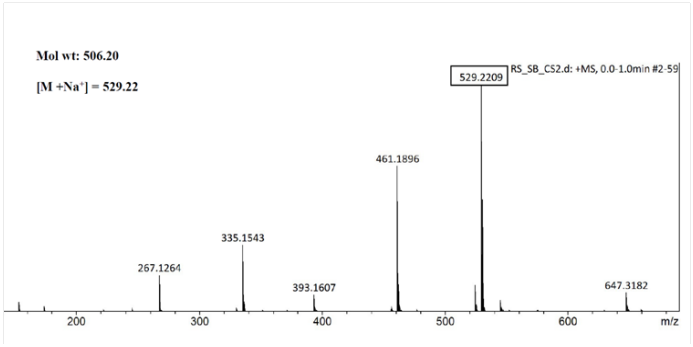

Figure S7 ESI-MS spectrum of compound 3.

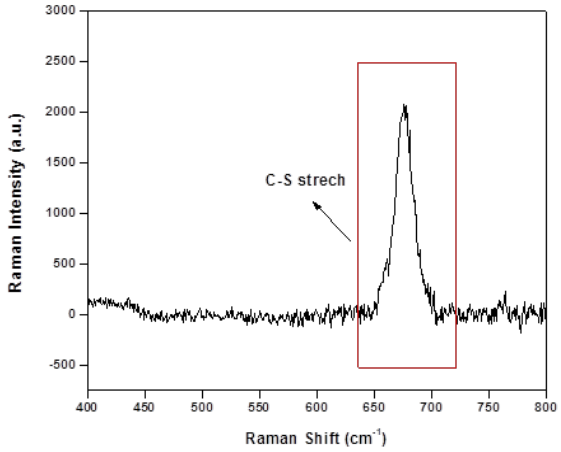

Figure S8 Raman Spectrum of the gel showing C-S stretching.

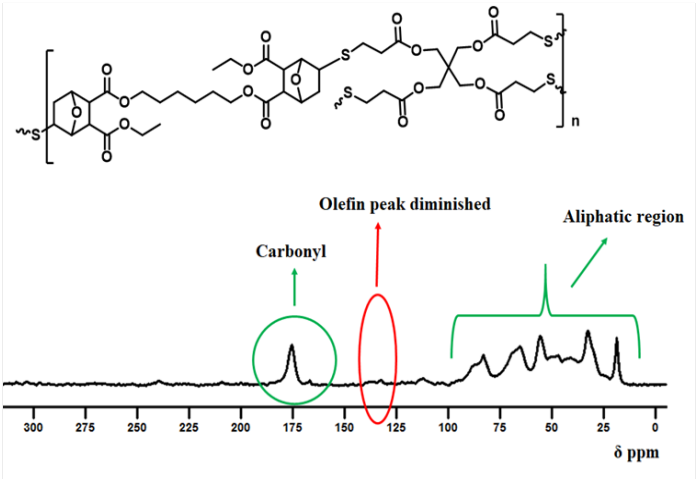

Figure S9 Cross-polarization (CP) ^{13}C MAS NMR spectrum of the gel.

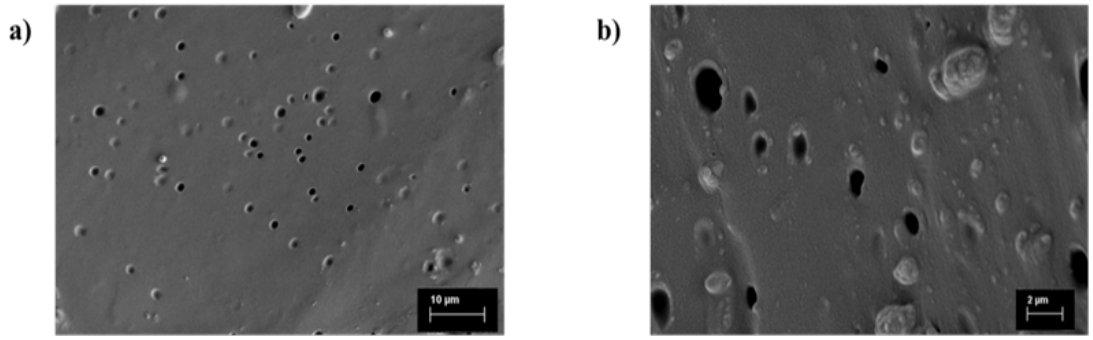

Figure S10 FE-SEM images of the gel at scale bar (A) 10µm and (B) 2µm respectively.

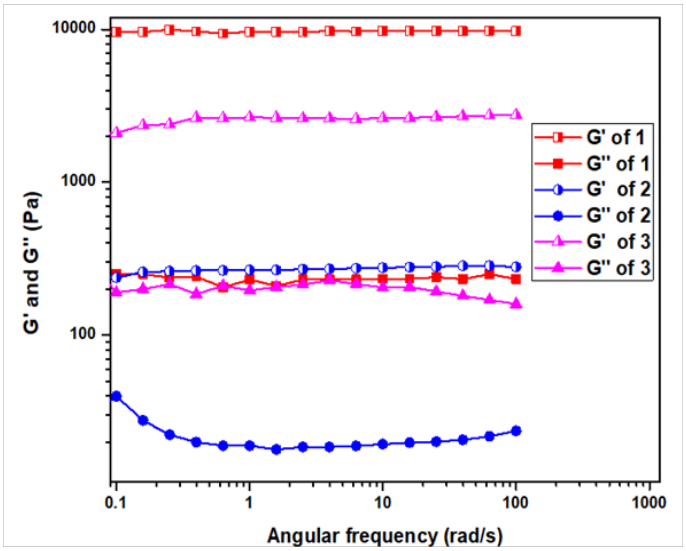

Figure S11 Storage modulus (G') and loss modulus (G") with varying angular frequency where 1, 2 and 3 represent thiol-norbornene feed ratio 1:2, 2:1 and 1.5:2 respectively.

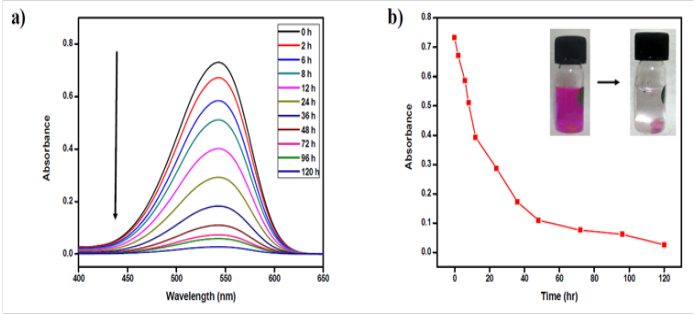

Figure S12 (A) UV-Vis spectra of dye Nile red (0.1mM) in DMF after the indicated hours. (B) plot of absorbance vs time; (inset picture shows removal of Nile red).

Transmission Electron Microscopy (TEM):

Microtomy analysis and imaging of the gel sample:

The medium (Epon_812 substitute), purchased from Sigma Aldrich, was used for embedding synthetic resin. The embedded resin was sliced at 30 nm thick films using microtome facility (Power Tome PC, RMC Boeckeler). The sliced film was dried under vacuum and was analysed using Transmission Electron Microscope; TEM (JEM-2100F) facility at 120 kV.

Tensile strength measurement: Tensile testing was performed on a Universal Testing Machine (DigiUTM, S. C. Dey & Co.) at a strain rate 1mm/min. at room temperature having dimension 25mm × 5mm × 0.2mm under a load 2KN. Five measurements have been done for each sample.

Thermo Gravimetric Analysis: Thermal studies were carried out using a Mettler Toledo TGA/SDTA 851e instrument at a heating rate of 10 ºC min^{-1}**(Table 4)**.

Table 4 Colour code

Grey	C
Sky blue	H
Red	O
Yellow	S
Violate	Na
Dark green	N
Light green	Cl

Conclusion

This report portrays the synthesis of an organogel based on photoinitiated thiol and biocompatible norbornene using click chemistry. Systematic characterisation was carried out by1H, 13C NMR, FT-IR spectroscopy as well as mass spectrometry. TEM analysis revealed the presence of uniform porous network on the surface. Good swelling capacity was observed in organic solvents such as DMSO, DMF, chloroform and DCM. Thermo Gravimetric Analysis revealed the ability of the gel to resist high temperature. Rheological measurements suggested presence of elasticity in the network structure. Tensile strength measurement suggested that the material under investigation possess subtle rigidity in its network. The kinetics of dye adsorption fitted well pseudo-second-order model and Langmuir adsorption isotherm model was best suited for the dye removal process. Furthermore, the organogel efficiently eliminated cationic toxic dyes from aqueous phase but did not take up much water itself during the removal process, thereby causing minimum waste of water. DFT calculations suggest the favourable interaction energy between the dyes and the gel as the defining parameter for the selective uptake of cationic dyes by the gel. The understanding of structure-

property relationship of this design holds the future prospective of wastewater treatment. Conclusively, this particular adsorbent is exclusive because of its bio-compatibility, ease of separation after adsorption and higher thermal and mechanical stability.

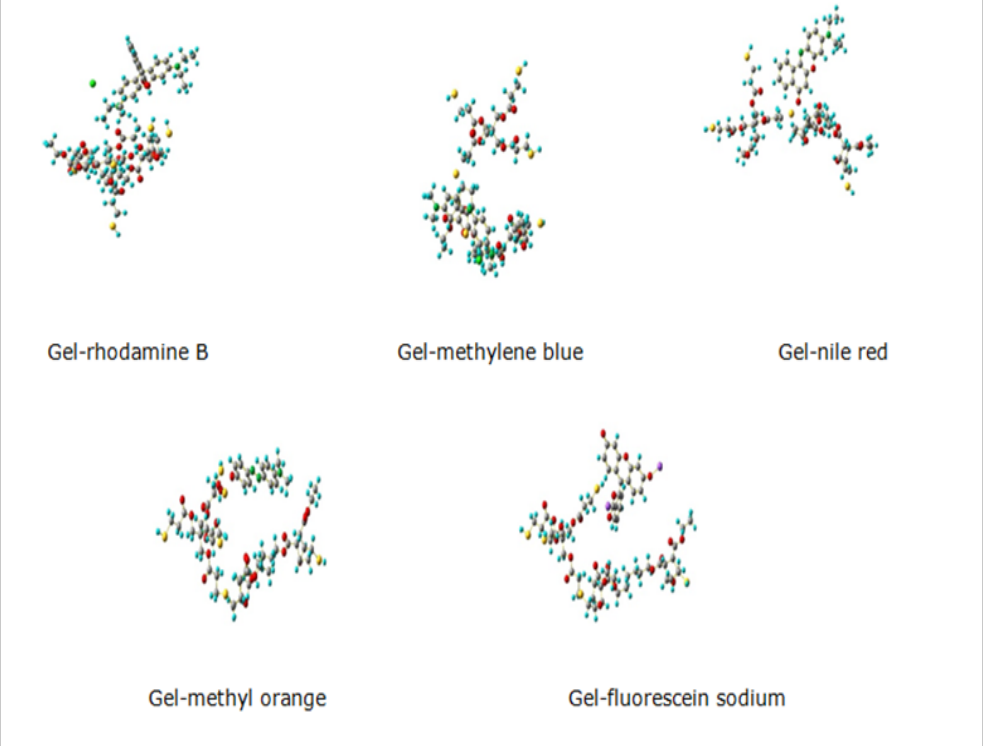

Figure S13 Optimised geometries of gel-dye complexes.

Conflicts of interest

There are no conflicts to declare.

Acknowledgments

S.B. thanks IISER Kolkata for research fellowship. A.N. thanks INSPIRE for fellowship. We thank Dr. M.M. for tensile strength measurement. R.S. thanks DST and DBT for funding. Authors thank IISER Kolkata for infrastructure.

References

1. Smith DK, Okesola BO. Applying low-molecular weight supramolecular gelators in an environmental setting-self-assembled gels as smart materials for pollutant removal. *Chem Soc Rev.* 2016;45(15):4226–4251.
2. Sehaqui H, Stefelova J, Slovak V, et al. Drying and pyrolysis of cellulose nanofibers from wood, bacteria, and algae for char application in oil absorption and dye adsorption. *ACS Sustainable Chem Eng.* 2017;5(3):267–2692.
3. Field RW. Surface science: separation by reconfiguration. *Nature* 2012;489(7414):4–42.
4. Ai L, Zhang C, Liao F, et al. Removal of methylene blue from aqueous solution with magnetite loaded multi-wall carbon nanotube: Kinetic, isotherm and mechanism analysis. *J Hazard Mater*. 2011;198:282–290.
5. Sun H, Cao L, Lu L. Magnetite/reduced graphene oxide nanocomposites: on step solvothermal synthesis and use as a novel platform for removal of dye pollutants. *Nano Res.*201;4(6):550–562.
6. Inbaraj BS, Chen BH. Dye adsorption characteristics of magnetite nanoparticles coated with a biopolymer poly(c-glutamic acid). *Bioresour Technol*. 2011;102(19):8868–8876.
7. Rakhshaee R, Panahandeh M. Stabilization of a magnetic nano-adsorbent by extracted pectin to remove methylene blue from aqueous solution: A comparative studying between two kinds of cross-likened pectin. *J Hazard Mater.* 2011;189(1-2):158–166.
8. Li S. Removal of crystal violet from aqueous solution by sorption into semi-interpenetrated networks hydrogels constituted of poly (acrylic acid-acrylamide-methacrylate) and amylose. *Bioresour Technol*. 2010;101(7):2197–2202.
9. Bao N, Li Y,Wei Z, et al. Adsorption of Dyes on Hierarchical Mesoporous TiO_2 Fibers and Its Enhanced Photocatalytic Properties. *J Phys Chem C*. 2011;115(13);5708–5719.
10. Salleh MAM, Mahmoud KD, Karim AWAW, et al. Cationic and anionic dye adsorption by agricultural solid wastes: A comprehensive review. *Desalination* 2011;280(1–3):1–13.
11. Kaur H, Kaur R. Removal of rhodamine-B dye from aqueous solution onto Pigeon Dropping: Adsorption, Kinetic, Equilibrium and Thermodynamic studies. *J Mater Environ Sci.* 2014;5(6):1830–1838.
12. Nebsen M, Attallah O, Al-Ghobashy AM, et al. Removal of cationic and anionic dyes from aqueous solution with magnetite/pectin and magnetite/silica/pectin hybrid nanocomposites: kinetic, isotherm and mechanism analysis. *RSC Advances*. 2016;6(14):11461–11480.
13. Gomes VG, Bustamante H, Rabines M. Operating strategies for acid phase digestion: an industrial case study. *Water Environ J.* 2016;30(1–3):227–234.

14. Liu Z, Gomes V, Zhou C, et al. Poly (vinylidene fluoride) / Polyaniline/ MWCNT nanocomposite ultrafiltration membrane for natural organic matter removal. *Separation and Purification Technology.* 2018;190(1):143–155.

15. Kunduru KR, Jana T, Kutcherlapati SNR, et al. Armored Urease: Enzyme-Bioconjugated Poly(acrylamide) Hydrogel as a Storage and Sensing Platform. *Methods Enzymol.* 2017;590:143–167.

16. Oh SY, Cha DK, Chiu PC, et al. Conceptual comparison of pink water treatment technologies: granular activated carbon, anaerobic fluidized bed, and zero-valent iron-Fenton process. *Water Sci Technol* 2004;49(5–6):129–136.

17. Perey JR1, Chiu PC, Huang CP, et al. Zero-Valent Iron Pretreatment for Enhancing the Biodegradability of Azo Dyes. *Water Environ Res.* 2002;74(3):221–225.

18. Yu L, Cheng N, Hu Q, et al. Efficient and Selective Removal of Dyes Using Imidazolium-Based Supramolecular Gels. *ACS Appl Mater Interfaces* 2015;7(19):10258–10265.

19. Li Q, Daikun L, Bai N, et al. One-Step Synthesis of Cationic Hydrogel for Efficient Dye Adsorption and Its Second Use for Emulsified Oil Separation. *ACS Sustainable Chem Eng.* 2017;5(6):5598–5607.

20. Kumar R, Shunmugam R. Unique Design of Porous Organic Framework Showing Efficiency toward Removal of Toxicants. *ACS Omega* 2017;2(8):4100–4107.

21. Mukherjee S, Shunmugam R. Polymer based Nano-Assemblies: Very Efficient Carrier in the Field of Cancer Chemotherapy. *J Nanomed Res*. 2017;5(6):00137.

22. Binder WH, Sachsenhofer R. 'Click' Chemistry in Polymer and Material Science: An Update. *Macromol Rapid Commun*. 2008;29(12-13):952–981.

23. Moses JE, Moorhouse AD. The growing applications of click chemistry. *Chem Soc Rev.* 2007;36(8):1249–1232.

24. Li M, De P, Gondi SR, et al. End Group Transformations of RAFT-Generated Polymers with Bismaleimides: Functional Telechelics and Modular Block Copolymers. *Journal of polymer science.* 2008;46(15):5093–5100.

25. Becer CR, Hoogenboom R, Schubert US. Click Chemistry beyond Metal-Catalyzed Cycloaddition. *Angew Chem Int Ed.* 2009;48(27):4900–4908.

26. Singh I, Zarafshani Z, Lutz JF, et al. Metal-Free "Click" Chemistry: Efficient Polymer Modification via 1, 3-Dipolar Cycloaddition of Nitrile Oxides and Alkynes. *Macromolecules.* 2009;42(15):5411–5413.

27. Yu B, Chan JW, Hoyle CE, et al. Sequential Thiol-Ene/Thiol-Ene and Thiol-Ene/Thiol-Yne Reactions as a Route to Well-Defined Mono and Bis End Functionalized Poly(N-isopropylacrylamide). *J Polym Sci Part A Polym Chem.* 2009;47(14):3544–3557.

28. Chan W, Hoyle CE, Lowe AB. Sequential Phosphine-Catalyzed, Nucleophilic Thiol-Ene/Radical-Mediated Thiol-Yne Reactions and the Facile Orthogonal Synthesis of Polyfunctional Materials. *J Am Chem Soc.* 2009;131(16):5751–5753.

29. Gress A, Volkel A, Schlaad H. Thio-Click Modification of Poly[2-(3-butenyl)-2-oxazoline]. *Macromolecules.* 2007;40(22):7928–7933.

30. Killops KL, Campos LM, Hawker CJ. Robust, Efficient, and Orthogonal Synthesis of Dendrimers via Thiol-ene "Click" Chemistry. *J Am Chem Soc.* 2008;130(15):5062–5064.

31. Chan JW, Yu B, Hoyle CE, et al. Convergent synthesis of 3-arm star polymers from RAFT-prepared poly(N,N-diethylacrylamide) via a thiol–ene click reaction. *Chem Commun.* 2008;(40):4959–4961.

32. Wei H, Senyurt AF, Jonsson S, et al. Photopolymerization of Ternary Thiol–Ene/Acrylate Systems: Film and Network Properties. *J Polym Sci Part A Polym Chem.* 2007;45(5):822–829.

33. Li Q, Zhou H, Hoyle CE, et al. Effects of Monomer Functionality and Hydrogen Bonding on the Polymerization Kinetics and Properties of Thiol-Ene Networks. *Macromolecules.* 2009;42(8):2994–2999.

34. Hoyle CE, Bowman CN. Thiol–Ene Click Chemistry. *Angew Chem Int Ed.* 2010;49(9):1540–1573.

35. Fairbanks DB, Schwartz PM, Halevi EA, et al. Versatile Synthetic Extracellular Matrix Mimic via Thiol-Norbornene Photopolymerization. *Adv Mater.* 2009;21(48):5005–5010.

36. Griesbaum K. Problems and Possibilities of the Free-Radical Addition of Thiols to Unsaturated Compounds. *Angew Chem Int Ed.* 1970;9(4):273–287.

37. Hoyle EC, Lee TY, Roper T. Thiol–Enes: Chemistry of the Past with Promise for the Future. *J Polym Sci Part A.* 2004;42(21):5301–5338.

38. Lowe BA. Thiol-ene ''click'' reactions and recent applications in polymer and materials synthesis: a first update. *Polym Chem.* 2014;5(17):4820–4870.

39. Shih H, Lin CC. Cross-Linking and Degradation of Step-Growth Hydrogels Formed by Thiol−Ene Photoclick Chemistry. *Biomacromolecules.* 2012;13(7):2003–2012.

40. Madkour E, Grolman JM, Tew GN. Synthesis of hydrogels via ring-opening metathesis polymerization: factors affecting gelation. *Polym Chem.* 2011;2(1):114–119.

41. Basak D, Das A, Ghosh S. Hydrogen-bonding driven luminescent assembly and efficient F¨orster Resonance Energy Transfer (FRET) in a dialkoxynaphthalene-based organogel. *RSC Adv*. 2014;4(82):43564–43571.

42. Mondal T, Ghosh S. One Pot Synthesis and Gelation Studies of Amphiphilic Triblock Polyurethanes. *Journal of Polymer Science Part A Polymer Chemistry.* 2014;52(17):2502–2508.

43. Ganivada MN, Kumar P, Shunmugam R. A unique polymeric gel by thiol–alkyne click chemistry. *RSC Adv.* 2015;5(62):50001–50004.

44. Khonakdar HA, Morshedian J, Wagenknecht U, et al. An investigation of chemical crosslinking effect on properties of high-density polyethylene. *Polymer.* 2003;44(15):4301–4309.

45. Haldar U, Nandi M, De P, et al. POSS-induced enhancement of mechanical strength in RAFT-made thermoresponsive hydrogels. *Polym Chem.* 2015;6(28):5077–585.

46. Roy SG, Haldar U, De P. Remarkable Swelling Capability of Amino Acid Based Cross-Linked Polymer Networks in Organic and Aqueous Medium. *ACS Appl Mater Interfaces.* 2014;6(17):4233–4241.

47. Haldar U, Bauri K, De P, et al. Polyisobutylene-Based pH-Responsive Self-Healing Polymeric Gels. *ACS Appl Mater Interfaces.* 2015;7(16):8779–8788.

48. Lawrenson S, Peigneguy F, North M, et al. Greener solvents for solid-phase synthesis. *Green Chem.* 2017;19(4):952–962.

49. Sarin KV, Merrifield RB, Kent SBH. Properties of Swollen Polymer Networks. Solvation and Swelling of Peptide-Containing Resins in Solid-Phase Peptide Synthesis. *J Am Chem Soc.* 1980;102(17):5463–5470.

50. Yang B, Zhao S, Tian, S. A study of thermal decomposition of alkanethiols in pressure reactor. *Fuel Process Technol.* 2006;87(8):673–678.

51. Li X, Yao H, Li Z, et al. Thermal Stability of Oxygen-Containing Functional Groups on Activated Carbon Surfaces in a Thermal Oxidative Environment. *Journal of chemical engineerin.* 2014;47(1):21–27.

52. Malkappa K, Jana T. Simultaneous Improvement of Tensile Strength and Elongation: An Unprecedented Observation in the Case of Hydroxyl Terminated Polybutadiene Polyurethanes. *Ind Eng Chem Res.* 2013;52(36):12887–12896.

53. Sharma N, Lakhman K, Kasi RM, et al. Physical Gels of [BMIM][BF4] by N-tert-Butylacrylamide/Ethylene Oxide Based Triblock Copolymer Self Assembly: Synthesis, Thermomechanical, and Conducting Properties. *J Appl Polym Sci.* 2013;128(6):3982–3992.

54. Zhou Y, Sharma N, Kasi RM, et al. Hierarchically Structured Free-Standing Hydrogels with Liquid Crystalline Domains and Magnetic Nanoparticles as Dual Physical Cross-Linkers. *J Am Chem Soc.* 2012;134(3):1630–1641.

55. Sun TL, Kurokawa T, Kuroda S, et al. Physical hydrogels composed of polyampholytes demonstrate high toughness and viscoelasticity. *Nat Mater.* 2013;12(10):932–937.

56. Zhang J, Guo DS, Liu Y, et al. Supramolecular binary hydrogels from calixarenes and amino acids and their entrapment–release of model dye molecules. *Soft Matter.* 2011;7(5):1756–1792.

57. Becker T, Goh YC, Jones F, et al. Proline-functionalised calix [4] arene: an anion-triggered hydrogelator. *Chem Commun.* 2008;(33):3900–3902.

58. Zheng YS, Song S, Wang J, et al. Supramolecular hydrogel based on amphiphilic calix [4] arene and its application in the synthesis of silica nanotubes. *RSC Adv.* 2014;4(47):24909–24913.

59. Boekhoven J, Poolman JM, Maity C, et al. Catalytic control over supramolecular gel formation. *Nature Chemistry.* 2013;5(5):433–437.

60. Tew GN, Cui J, Lackey MA, et al. Synthetically Simple, Highly Resilient Hydrogels. *Biomacromolecules.* 2012;13(3):584–588.

61. El-Nasr A, Ayad MM. Adsorption of Cationic Dye (Methylene Blue) from Water Using Polyaniline Nanotubes Base. *J Phys Chem C.* 2010;114(34):14377–17383.

62. Li Q, Li D, Bai N, et al. One-Step Synthesis of Cationic Hydrogel for Efficient Dye Adsorption and Its Second Use for Emulsified Oil Separation. *ACS Sustainable Chem Eng.* 2017;5(6):5598–5607.

63. Becke AD. Density-functional exchange-energy approximation with correct asymptotic behavior. *Phys Rev A.* 1988;38(6):3098–3100.

64. Frisch MJ, Trucks GW, Schlegel HB, et al. Gaussian 09 Citation. *Expanding the limits of computational chemistry*. 2009.

Citation: Bhattacharya S, Nair A, Bag A, et al. Engineering photo cross-linked porous network for efficient and selective removal of toxicants from wastewater. *MOJ Research Review.* 2019;2(2):69–81. DOI: 10.15406/mojcrr.2019.02.00058